J|A|C|S
ARTICLES
Published on Web 10/19/2006

DNA Condensation and Cell Transfection Properties of Guanidinium Calixarenes: Dependence on Macrocycle Lipophilicity, Size, and Conformation

Francesco Sansone,[†] Miroslav Dudič,[†] Gaetano Donofrio,[‡] Claudio Rivetti,[§] Laura Baldini,[†] Alessandro Casnati,[†] Sara Cellai,[§] and Rocco Ungaro*,[†]

Contribution from the Dipartimento di Chimica Organica e Industriale, Università degli Studi, Viale G. P. Usberti 17/A, 43100 Parma and Consorzio INSTM, Via Giusti 9, 50121 Firenze, Italy, Dipartimento di Salute Animale, Università degli Studi, Via del Taglio 8, 43100 Parma, Italy, and Dipartimento di Biochimica e Biologia Molecolare, Università degli Studi, Viale G. P. Usberti 23/A, 43100 Parma, Italy

Received May 17, 2006; E-mail: rocco.ungaro@unipr.it

Abstract: Calix[*n*]arenes functionalized with guanidinium groups at the upper rim and alkyl chains at the lower rim bind to DNA, condense it, and in some cases, promote cell transfection depending on their structure and lipophilicity. Atomic force microscopy (AFM) studies indicate that upon DNA binding the hydrophobic association of the lipophilic chains of cone guanidinium calix[4]arenes drives the formation of intramolecular DNA condensates, characterized by DNA loops emerging from a dense core. Furthermore, hexyl and octyl chains confer to these calixarenes cell transfection capabilities. Conversely, larger and conformationally mobile calix[6]- and calix[8]arene methoxy derivatives form intermolecular aggregates characterized by "gorgonlike" structures composed of multiple plectomenes. These adducts, in which interstrand connections are dominated by electrostatic interactions, fail to promote cell transfection. Finally, calix[4]arenes in a 1,3-alternate conformation show an intermediate behavior because they condense DNA, but the process is driven by charge−charge interactions.

Introduction

Gene therapy can be defined as the delivery of nucleic acids to cells with a vector for some therapeutic purpose.[1] Both viral[2] and nonviral[3] vectors have been proposed, and the latter are receiving more and more attention because of the concerns associated with the use of recombinant viruses. Among the synthetic vectors, cationic lipids,[4] gemini surfactants,[5] and other cationic polyelectrolites such as poly(L-lysine),[6] polyethylenimines,[7] and polyamine dendrimers[8] have been thoroughly investigated. Quite recently, very promising neutral macrocyclic sugar conjugates, known as glycocluster nanoparticles (GNPs), have been shown to condense plasmid DNA thus mediating transfection of cells in vitro.[9] Also, the guanidinium group, which is very well-known to bind small anionic substrates[10] and has been incorporated into several synthetic receptors for this purpose,[11] has been used for the recognition of (poly)nucleotides[12] and proteins.[13] In few cases, the guanidinium-based ligands were shown to penetrate cells[14] or promote efficient gene transfection.[15]

We recently reported the synthesis of calix[*n*]arenes **4G4Pr-*cone***, **4G4Oct-*cone***, **6G6Me-*mobile***, and **8G8Me-*mobile*** (see Chart 1) bearing guanidinium groups at the upper rim (aromatic rings) together with very preliminary data on their DNA binding properties.[17] The results were particularly attractive because they

[†] Dipartimento di Chimica Organica e Industriale.
[‡] Dipartimento di Salute Animale.
[§] Dipartimento di Biochimica e Biologia Molecolare.

(1) Niculescu-Duvaz, I.; Spooner, R.; Marais, R.; Springer, C. J. S. *Bioconjugate Chem.* **1998**, *9*, 4−22.
(2) Crystal, R. G. *Science* **1995**, *270*, 404−410.
(3) Zuber, G.; Dauty, E.; Nothisen, M.; Belguise, P.; Behr, J.-P. *Adv. Drug. Delivery Rev.* **2001**, *52*, 245−253.
(4) Sainlos, M.; Hauchecorne, M.; Oudrhiri, N.; Zertal-Zidani, S.; Aissaoui, A.; Vigneron, J.-P.; Lehn, J.-M.; Lehn, P. *Chem. Bio. Chem.* **2005**, *6*, 1023−1033.
(5) Kirby, A. J. et al. *Angew. Chem., Int. Ed.* **2003**, *42*, 1448−1457.
(6) Okuda, T.; Kidoaki, S.; Ohsaki, M.; Koyama, Y.; Yoshikawa, K.; Niidome, T.; Aoyagi, H. *Org. Biomol. Chem.* **2003**, *1*, 1270−1273.
(7) Kichler, A. *J. Gene Med.* **2004**, *6*, S3−S10.
(8) Guillot, M.; Eisler, S.; Weller, K.; Merkle, H. P.; Gallani, J.-L.; Diederich, F. *Org. Biomol. Chem.* **2006**, *4*, 766−769.
(9) Nakai, T.; Kanamori, T.; Sando, S.; Aoyama, Y. *J. Am. Chem. Soc.* **2003**, *125*, 8465−8475.
(10) (a) Müller, G.; Riede, J.; Schmidtchen, F. P. *Angew. Chem., Int. Ed. Engl.* **1988**, *27*, 1516−1518. (b) Echavarren, A.; Galán, A.; Lehn, J.-M.; de Mendoza, J. *J. Am. Chem. Soc.* **1989**, *111*, 4994−4995. (c) Hannon, C. L.; Anslyn, E. V. In *Bioorganic Chemistry Frontiers*; Dugas, H., Schmidtchen, F. P., Eds; Springer Publishers: Berlin, 1993; Vol. 3, pp 193−255. (d) Schug, K. A.; Lindner, W. *Chem. Rev.* **2005**, *105*, 67−113. (e) Schmuck, C.; Geiger, L. *Chem. Commun.* **2005**, 772−774.
(11) (a) Seel, C.; Galán, A.; de Mendoza, J. *Top. Curr. Chem.* **1995**, *175*, 101−132. (b) Berger, M.; Schmidtchen, F. P. *Chem. Rev.* **1997**, *97*, 1609−1646. (c) Orner, B. P.; Hamilton, A. D. *J. Incl. Phenom. Macrocycl. Chem.* **2001**, *41*, 141−147. (d) Houk, R. J. T.; Tobey, S. L.; Anslyn, E. V. *Top. Curr. Chem.* **2005**, *255*, 199−229.
(12) (a) Andreu, C.; Galán, A.; Kobiro, K.; de Mendoza, J.; Park, T. K.; Rebek, J., Jr.; Salmeron, A.; Usman, N. *J. Am. Chem. Soc.* **1994**, *116*, 5501−5502. (b) Perreault, D. M.; Cabell, L. A.; Anslyn, E. V. *Bioorg. Med. Chem.* **1997**, *5*, 1209−1220.
(13) Salvatella, X.; Martinell, M.; Gairí, M.; Mateu, M. G.; Feliz, M.; Hamilton, A. D.; de Mendoza, J.; Giralt, E. *Angew. Chem., Int. Ed.* **2004**, *43*, 196−198.
(14) (a) Fernández-Carneado, J.; Van Gool, M.; Martos, V.; Castel, S.; Prados, P.; de Mendoza, J.; Giralt, E. *J. Am. Chem. Soc.* **2005**, *127*, 869−874. (b) Jones, L. R.; Goun, E. A.; Shinde, R.; Rothbard, J. B.; Contag, C. H.; Wender, P. A. *J. Am. Chem. Soc.* **2006**, *128*, 6526−6527.

10.1021/ja0634425 CCC: $33.50

Chart 1. Structure of the Guanidinium Calixarenes[a]

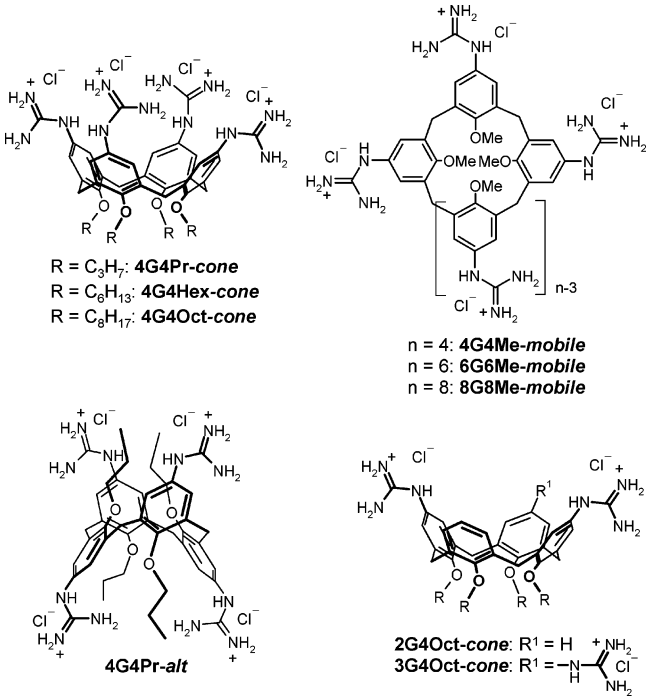

[a] To facilitate the reader in identifying the structure of the calixarene ligands, we introduced in the text the running nomenclature **mG*n*alk-*conf*** where **mG** indicates the number of the guanidinium units, ***n*** is the size of the calix[*n*]arene (calix[4]-, -[6]-, or -[8]arene), **alk** is the alkyl chain (methyl, propyl, hexyl, octyl) at the lower rim and ***conf*** is the conformation assumed by the macrocycle (cone, 1,3-alternate, mobile).[16]

suggested the possibility of using these compounds as novel cationic synthetic vectors for DNA. The high synthetic versatility of the calixarene platform offers the unique opportunity of tuning the DNA binding capability, by changing the number of charged guanidinium groups at the upper rim, and the conformational properties and lipophilicity of the vector, by changing the nature and the length of the alkyl substituents on the phenolic OH groups at the lower rim.

Therefore, we have synthesized new guanidinium calix[4]-arenes (**4G4Hex-*cone***, **4G4Pr-*alt***, **4G4Me-*mobile***, **2G4Oct-*cone***, and **3G4Oct-*cone***; see Chart 1) and, together with the above-mentioned derivatives, evaluated their DNA binding and transfection properties using spectroscopic measurements, atomic force microscopy (AFM) visualization, and transfection experiments.

Results

Synthesis, Conformation, and Self-Aggregation of Guanidinium Calixarenes. Synthesis of the **4G4Hex-*cone***, **4G4Pr-*alt***, and **4G4Me-*mobile*** derivatives, functionalized at the upper rim with four guanidinium groups, started from the tetra-*tert*-butyl-calix[4]arene (Scheme 1) which was alkylated using established procedures to obtain the cone isomer **1a**,[18] the conformationally mobile **1c**,[19] and the 1,3-alternate calix[4]arene **1b**.[20] Subsequently, compounds **1a**−**c** were treated with $NaNO_3$ and CF_3COOH to substitute the *tert*-butyl with nitro groups through an *ipso*-nitration reaction (**2a**,[18] **2b**, and **2c**). Reduction to the corresponding tetramino intermediates **3a**,**b**,[21]**c** was then carried out, followed by reaction with di-Boc-protected thiourea units in the presence of Mukaiyama's reagent[22] or, alternatively, $HgCl_2$, which afforded compounds **4a**−**c**. Removal of the protecting groups gave tetraguanidinium macrocycles **4G4Hex-*cone***, **4G4Pr-*alt***, and **4G4Me-*mobile***.

Scheme 1 [a]

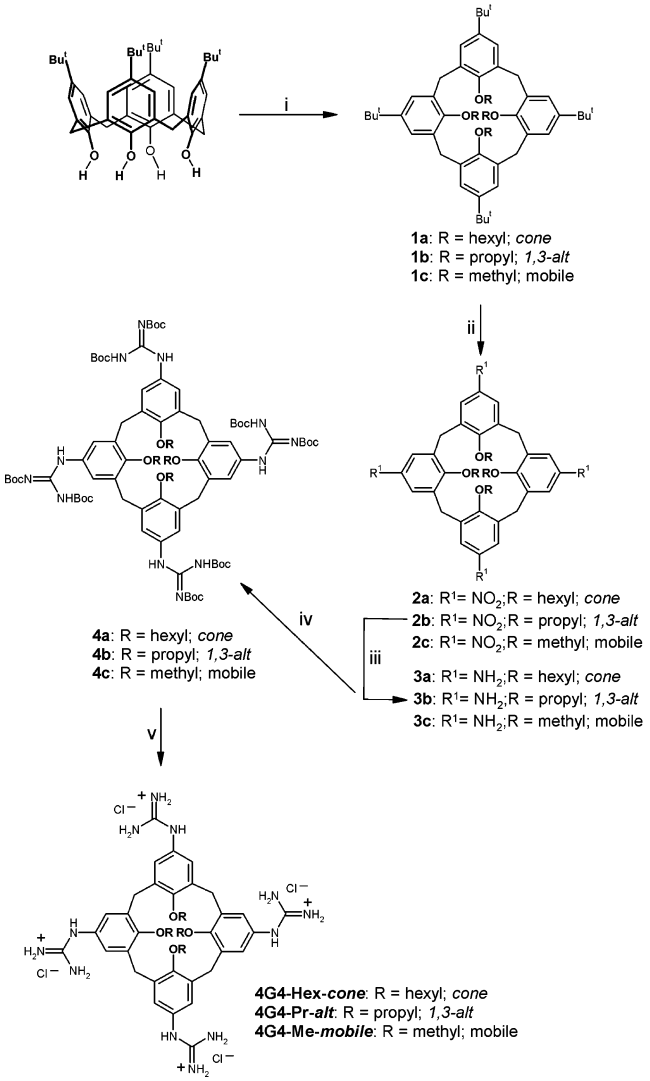

[a] Reagents and conditions: (i) RI, NaH in DMF, rt (to obtain compounds **1a**,**c**), or Cs_2CO_3 in CH_3CN, reflux (to obtain compound **1b**); (ii) $NaNO_3$/CF_3COOH; (iii) $NH_2NH_2{\cdot}H_2O$, Pd/C (10%) in EtOH or in $CH_3OCH_2CH_2OH$, reflux; (iv) Boc-NH-C(S)-NH-Boc, $HgCl_2$ in DMF or Mukaiyama's reagent in CH_2Cl_2; (v) concentrated HCl/1,4-dioxane.

(15) (a) Patel, M.; Vivien, E.; Hauchecorne, M.; Oudrhiri, N.; Ramasawmy, R.; Vigneron, J.-P.; Lehn, P.; Lehn, J.-M. *Biochem. Biophys. Res. Commun.* **2001**, *281*, 536−543. (b) Aissaoui, A.; Oudrhiri, N.; Petit, L.; Hauchecorne, M.; Kan, E.; Sainlos, M.; Julia, S.; Navarro, J.; Vigneron, J.-P.; Lehn, J.-M.; Lehn, P. *Curr. Drug Targets* **2002**, *3*, 1−16. (c) Luton, D.; Oudrhiri, N.; de Lagausie, P.; Aissaoui, A.; Hauchecorne, M.; Julia, S.; Oury, J.-F.; Aigrain, Y.; Peuchmaur, M.; Vigneron, J.-P.; Lehn, J.-M.; Lehn, P. *J. Gene Med.* **2004**, *6*, 328−336. (d) Martin, B.; Sainlos, M.; Aissaoui, A.; Oudrhiri, N.; Hauchecorne, M.; Vigneron, J.-P.; Lehn, J.-M.; Lehn, P. *Curr. Pharm. Des.* **2005**, *11*, 375−394.
(16) Gutsche, C. D. In *Calixarenes Revisited: Monographs in Supramolecular Chemistry*; The Royal Society of Chemistry: Cambridge, 1998.
(17) Dudič, M.; Colombo, A.; Sansone, F.; Casnati, A.; Donofrio, G.; Ungaro, R. *Tetrahedron* **2004**, *60*, 11621−11626.
(18) Kenis, P. J. A.; Noordman, O. F. J.; Schonherr, H.; Kerver, E. G.; Snellink-Ruel, B. H. M.; Van Hummel, G. J.; Harkema, S.; Van Der Vorst, C. P. J. M.; Hare, J.; Picken, S. J.; Engbersen, J. F. J.; Van Hulst, N. F.; Vancso, G. J.; Reinhoudt, D. N. *Chem.−Eur. J.* **1998**, *4*, 1225−1234.
(19) Gutsche, C. D.; Dhawan, B.; Levine, J. A.; Hyun No, K.; Bauer, L. J. *Tetrahedron* **1983**, *39*, 409−426.
(20) Iwamoto, K.; Araki, K.; Shinkai, S. *J. Org. Chem.* **1991**, *56*, 4955−4962.
(21) Mislin, G.; Graf, E.; Hosseini, M. W. *Tetrahedron Lett.* **1996**, *37*, 4503−4506.
(22) Mukaiyama, T. *Angew. Chem., Int. Ed. Engl.* **1979**, *18*, 707−721.

1,3-Di- (**2G4Oct-*cone***) and triguanidiniumcalix[4]arenes (**3G4Oct-*cone***) with octyl chains at the lower rim, both blocked in the cone conformation, were synthesized with a similar procedure starting from the de-*tert*-butylated calix[4]arene. Unfortunately, they are completely insoluble in water which hindered further studies. Therefore, the synthesis and characterization of these compounds are reported in Supporting Information together with the reaction scheme (Figure S1).

We have previously shown[17] that calixarenes **6G6Me-*mobile*** and **8G8Me-*mobile*** are water soluble and do not self-associate in this solvent. In the new series of macrocycles, the conformationally mobile **4G4Me-*mobile*** adopts a 1,3-alternate structure as inferred by the presence of a singlet at 3.73 ppm and a signal at 38.5 ppm in ^{1}H and ^{13}C NMR spectra, respectively. These signals refer to all bridging methylene groups and are diagnostic for this conformation,[23] as also confirmed by the very similar spectral features shown by **4G4Pr-*alt*** which is blocked in the 1,3-alternate conformation. As previously observed for other water-soluble calix[4]arenes,[24] the exposure of the lipophilic groups to the solvent is minimized for derivatives in the 1,3-alternate conformation, thus both the **4G4Me-*mobile*** and **4G4Pr-*alt*** ligands do not self-aggregate in the concentration range $10^{-5}-10^{-2}$ M. Conversely, the cone calix[4]arenes tend to aggregate, although to a minor extent if compared to other similar water-soluble calix[4]arene derivatives. In fact, **4G4Pr-*cone*** does not aggregate up to its solubility limit (10^{-2} M) whereas the corresponding tetrasulfonate[24] or tetracarboxylate[25] derivatives show a critical micellar concentration (cmc) of 2.5×10^{-3} and 6.5×10^{-5} M, respectively. Other cone tetrapropoxycalix[4]arenes having four quaternary ammonium groups at the upper rim show a cmc between 5.5×10^{-7} and 10^{-3} M.[26,27] **4G4Oct-*cone*** shows very little solubility in water,[17] whereas **4G4Hex-*cone*** shows a quite unique behavior which was studied in more detail. The ^{1}H NMR spectrum of this compound at 0.2 mM in D_2O at 298 K (Supporting Information, Figure S2a) shows one set of sharp signals with the multiplicity expected for a symmetrically functionalized calix[4]arene in the cone conformation. Increasing the macrocycle concentration results in the appearance of new broad resonances for the axial protons of the $-CH_2-$ bridge, the $-OCH_2-$, and the aromatic protons, which are upfield shifted and in slow exchange (on the NMR time scale) with the sharp signals. These new resonances can be reasonably attributed to the formation of aggregates of higher molecular weight, most probably micelles. By further increasing the concentration, while the intensity of the new broad signals increases, that of the sharp signals gradually decreases. At 1 mM, the signals corresponding to the two species are almost equally intense, whereas at 5 mM, only the broad signals are visible. This behavior is peculiar because it has never been observed for water-soluble calixarenes, where the different species in equilibrium are in a fast exchange regime (on the NMR time scale). Analysis of these data (Supporting Information, Figure S3) allowed us to evaluate a cmc of 2.0×10^{-4} M for this aggregated species in water.

To get more information on this point, we used diffusion-ordered 2D NMR spectroscopy (DOSY)[28] which is a useful method to study aggregation phenomena, as the diffusion coefficient (D) is related to the effective size and shape of the molecular species in solution. Because there is a partial overlap of the signals of **4G4Hex-*cone*** at 1 mM (Supporting Information, Figure S4b), we determined the hydrodynamic radius r_H of the two species on the 0.2 and 10 mM solutions (Supporting Information, Figure S4a,c). The values obtained ($r_H = 8.9$ and 32.7 Å, respectively) confirm that at 0.2 mM **4G4Hex-*cone*** is essentially present in a monomeric form (the length of the long axis of **4G4Hex-*cone*** in an extended conformation is ~19 Å, as estimated by molecular modeling), and at 10 mM, it assembles in large aggregates. The r_H of **4G4Pr-*cone*** determined by ^{1}H DOSY experiments does not significantly depend on the concentration ($r_H = 8.1$ and 9.3 Å for the 0.5 and 10 mM samples, respectively) and confirms the presence of a monomeric species (the length of the long axis of **4G4Pr-*cone*** is ~16 Å).

Interaction of Guanidinium Calixarenes with DNA. Preliminary evidence of the guanidinium calixarene's ability to bind DNA was obtained by electrophoresis mobility shift assays (EMSA),[17] revealing that the cone calix[4]arenes profoundly affect DNA conformation compared to other guanidinium calixarene ligands. Herein, we corroborated these binding capabilities with DNA melting assays and ethidium bromide (EtBr) displacement assays, conveniently used to assess DNA binding of other cationic amphiphiles.[29] Namely, DNA melting curves of linearized pEGFP-C1 plasmid[30] suggest that **4G4Pr-*cone*** and **4G4Pr-*alt*** significantly stabilize the double helix, whereas **8G8Me-*mobile*** assists strand dissociation (Supporting Information, Figure S5). Likewise, **4G4Pr-*cone***, **8G8Me-*mobile***, and **4G4Pr-*alt*** displace EtBr from the corresponding circular plasmid in a concentration-dependent manner but with very different curve profiles (Supporting Information, Figure S6). The more rapid, although partial, release of EtBr observed upon addition of **8G8Me-*mobile*** can be related to the double helix destabilization induced by this calixarene. Although these experiments confirm a different mode of interaction with DNA by the different calixarenes, they did not provide a clear picture of the binding phenomena.

To get further insight into the DNA structural changes induced by calixarene binding, we employed AFM.[31,32] This technique has been successfully used to study the interaction of both synthetic ligands[33] and proteins[34] with DNA. AFM experiments were carried out using both circular and linear DNA imaged in air with the tapping mode. Samples were prepared as described in the Experimental Section. Figure 1a shows a typical image of the 4731 bp long DNA plasmids deposited in the absence of calixarenes onto freshly cleaved mica. Single plasmids and

(23) Jaime, C.; de Mendoza, J.; Prados, P.; Nieto, P. M.; Sanchez, C. *J. Org. Chem.* **1991**, *56*, 3372−3376.
(24) Shinkai, S.; Arimura, T.; Araki, K.; Kawabata, H. *J. Chem. Soc., Perkin Trans. 1* **1989**, 2039−2045.
(25) Michels, J. J.; Huskens, J.; Engbersen, J. F. J.; Reinhoudt, D. N. *Langmuir* **2000**, *16*, 4864−4870.
(26) Arimori, S.; Nagasaki, T.; Shinkai, S. *J. Chem. Soc., Perkin Trans. 2* **1995**, 679−683.
(27) Arimori, S.; Nagasaki, T.; Shinkai, S. *J. Chem. Soc., Perkin Trans. 1* **1993**, 887−889.
(28) Cohen, Y.; Avram, L.; Frish, L. *Angew. Chem., Int. Ed.* **2005**, *44*, 520−554.
(29) Hyvönen, Z.; Plotniece, A.; Reine, I.; Chekavichus, B.; Duburs, G.; Urtti, A. *Biochim. Biophys. Acta* **2000**, *1509*, 451−466.
(30) Borovik, A. S.; Kalambet, Y. A.; Lyubchenko, Y. L.; Shitov, V. T.; Golovanov, E. I. *Nucleic Acid Res.* **1980**, *8*, 4165−4184.
(31) Bustamante, C.; Rivetti, C. *Annu. Rev. Biophys. Biomol. Struct.* **1996**, *25*, 395−429.
(32) Hansma, H. G. *Annu. Rev. Phys. Chem.* **2001**, *52*, 71−92.
(33) Volcke, C.; Pirotton, S.; Grandfils, Ch.; Humbert, C.; Thiry, P. A.; Ydens, I.; Dubois, P.; Raes, M. *J. Biotechnol.* **2006**, *125*, 11−21.
(34) Ceci, P.; Cellai, S.; Falvo, E.; Rivetti, C.; Rossi, G. L.; Chiancone, E. *Nucleic Acids Res.* **2004**, *32*, 5935−5944.

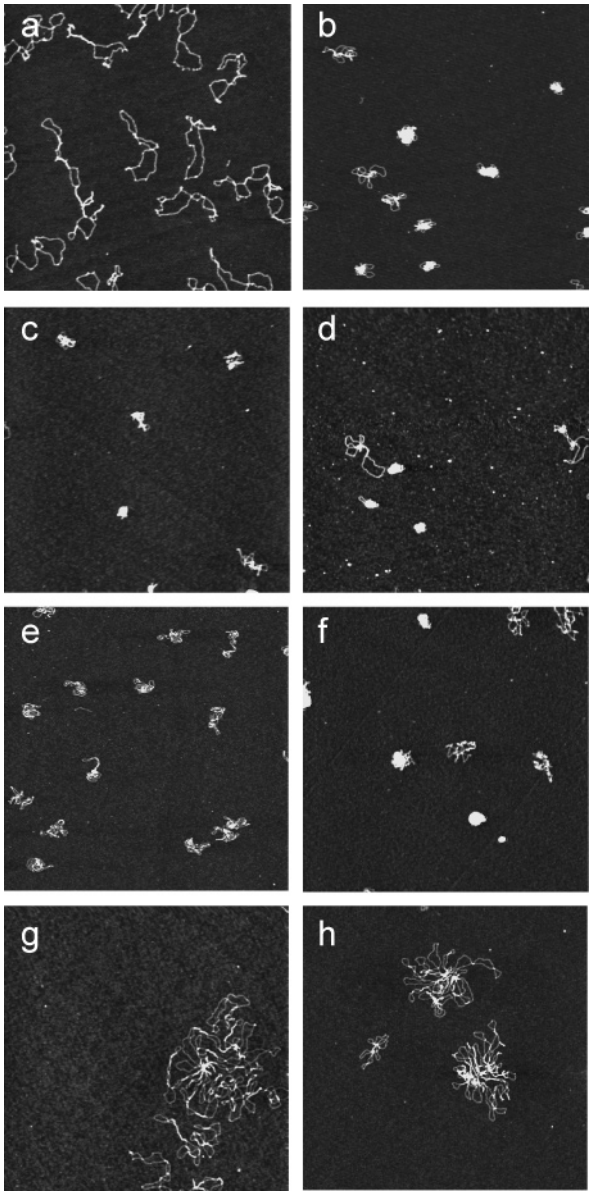

Figure 1. AFM images showing the DNA condensation induced by guanidinium calixarenes. All images were obtained with supercoiled pEGFP-C1 plasmid deposited onto mica at a concentration of 1 nM and with the microscope operating in the tapping mode in air. (a) Plasmid with no calixarenes added. Plasmid incubated with (b) 1 μM **4G4Pr-*cone***; (c) 1 μM **4G4Hex-*cone***; (d) 1 μM **4G4Oct-*cone***; (e) 1 μM **4G4Me-*mobile***; (f) 10 μM **4G4Pr-*alt***; (g) 1 μM **6G6Me-*mobile***; and (h) 1 μM **8G8Me-*mobile***. Each image represents a 2×2 μm scan.

concatamers are seen in their plectonemic form with several supercoils which cause the double helix to cross itself a number of times. Besides the topological constraint, plectonemes appear well extended all over the mica surface. The picture drastically changes when the DNA plasmid is incubated with calixarenes **4G4Pr-*cone*** (Figure 1b), **4G4Hex-*cone*** (Figure 1c), or **4G4Oct-*cone*** (Figure 1d) at a concentration of 1 μM. In these cases, the plasmids appear in highly condensed conformations with loops emerging from a dense core. Moreover, the dimension of the condensed structures suggests that, in the majority of the cases, they correspond to collapsed single DNA plasmids thus excluding the formation of large intermolecular aggregates. The DNA condensation induced by these calixarenes is concentration dependent as evidenced by a titration experiment (Supporting Information, Figure S7) in which the 4731 bp DNA plasmid was treated with increasing amounts of **4G4Pr-*cone*** ranging from 0.05 to 5 μM. Although at 0.05 μM **4G4Pr-*cone***, the conformation of the plasmid is unaffected by the calixarene, at 5 μM **4G4Pr-*cone***, most of the plasmids are highly condensed into large blobs. Higher calixarene concentrations could not be explored by AFM because they prevent DNA deposition onto the mica surface.

Similarly, **4G4Me-*mobile*** calix[4]arene, which as shown above adopts a 1,3-alternate conformation in solution, condenses DNA at a concentration of 1 μM (Figure 1e). On the other hand, **4G4Pr-*alt***, a conformer of **4G4Pr-*cone*** with the same conformation adopted by **4G4Me-*mobile***, does not bind DNA at 1 μM even though condensed filaments were observed at a concentration of 10 μM (Figure 1f).

A completely different picture emerges from the experiments performed with the conformationally mobile calix[6]- (**6G6Me-*mobile***) and calix[8]arene (**8G8Me-*mobile***) derivatives. As illustrated in Figure 1g,h, the DNA aggregation induced by these two calixarenes, at a concentration of 1 μM, results in the formation of interstrand aggregates composed of many plectonemes. These "gorgonlike", large DNA aggregates do not collapse into compact structures even at higher calixarene concentrations (data not shown).

Aggregates similar to those observed with circular DNA were also observed with 1200 bp linear DNA (Supporting Information, Figure S8), thus confirming that calixarene-induced DNA condensation is not coupled to the topological constraint of the plasmids.

Because all calixarenes studied contain aliphatic groups at the lower rim, it was of interest to investigate their DNA binding and condensation capabilities in a medium with a lower polarity. In Figure 2, representative AFM images of these experiments are reported. Plasmid DNA deposited onto mica in a buffer solution containing 5% (v/v) ethanol (Figure 2a) displays plectonemic conformations typical of supercoiled plasmids and comparable to those obtained in a buffer solution without ethanol. As shown in Figure 2b, however, under these conditions, the addition of 1 μM **4G4Pr-*cone*** does not generate the highly condensed structures seen before in the absence of ethanol and all deposited plasmids appear in extended plectonemic conformations. A strongly diminished capability to condense DNA in the presence of ethanol was also found for **4G4Hex-*cone*** and **4G4Oct-*cone*** calixarenes, although even at 15% EtOH not all plasmids are totally relaxed (Figure 2c,d). Conversely, the DNA binding properties of **4G4Me-*mobile***, **6G6Me-*mobile***, and **8G8Me-*mobile*** are not affected by the presence of the alcohol (Figure 2e−g), whereas the DNA condensation efficiency of **4G4Pr-*alt***, which is negligible in water at 1 μM, is significantly enhanced in 10% (v/v) ethanol (Figure 2h).

Transfection Properties of Guanidinium Calixarenes. The observation that several guanidinium calixarenes are able to condense DNA prompted us to explore the possibility of testing this class of macrocycles as vectors for cell transfection. By using the same DNA plasmid (pEGFP-C1) as that employed in the AFM studies, transfection experiments with the human rhabdomyosarcoma cell line RD-4 were carried out as described in the Experimental Section. This plasmid encodes for the enhanced green fluorescence protein whose expression can be used to monitor transfection efficiency by fluorescence micros-

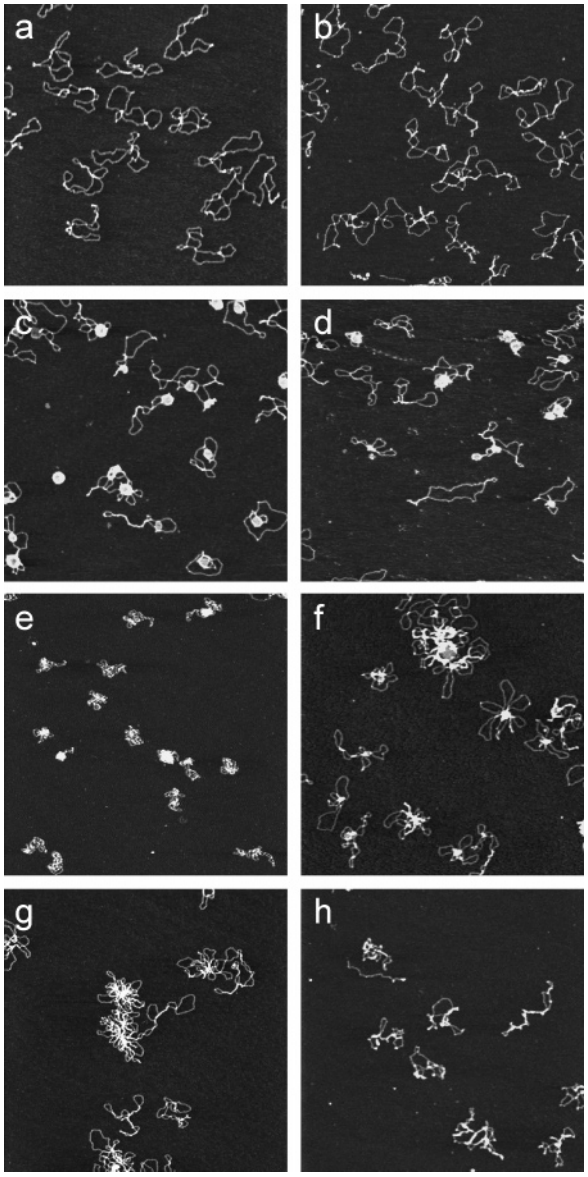

Figure 2. AFM images showing the effect of ethanol on calixarene-induced DNA condensation. Images of supercoiled pEGFP-C1 plasmid deposited onto mica at a concentration of 1 nM in buffer containing (a) 5% (v/v) ethanol; (b) 5% (v/v) ethanol and 1 μM **4G4Pr-*cone***; (c) 15% (v/v) ethanol and 1 μM **4G4Hex-*cone***; (d) 15% (v/v) ethanol and 1 μM **4G4Oct-*cone***; (e) 5% (v/v) ethanol and 1 μM **4G4Me-*mobile***; (f) 5% (v/v) ethanol and 1 μM **6G6Me-*mobile***; (g) 5% (v/v) ethanol and 1 μM **8G8Me-*mobile***; and (h) 10% (v/v) ethanol and 1 μM **4G4Pr-*alt***. Each image represents a 2 $\times$ 2 μm scan.

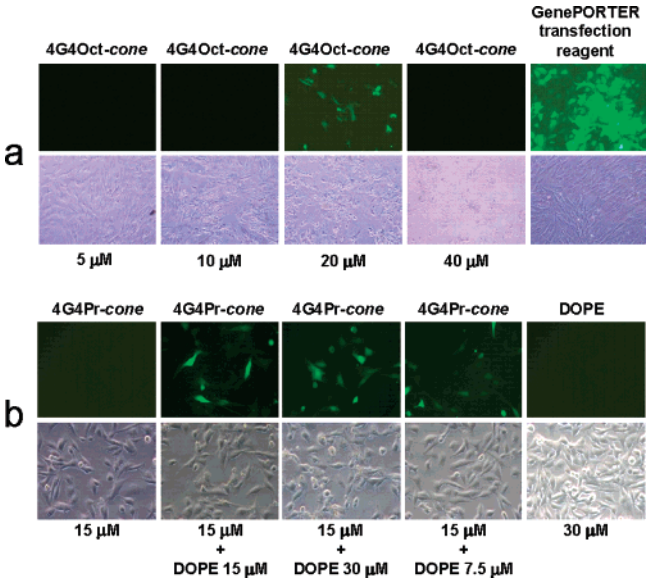

Figure 3. Transfection experiments with guanidinium calixarenes. (a) Cells transfected with **4G4Oct-*cone*** at the concentration indicated below each panel and visualized with fluorescence microscopy (upper row, in light green because they express the enhanced green fluorescence protein EGFP) and phase contrast microscopy (lower row). In the last column, the control experiment was performed with the GenePORTER transfection reagent. (b) Cells transfected with **4G4Pr-*cone*** at the concentration indicated below each panel in the absence and in the presence of DOPE and visualized with fluorescence microscopy (upper row) and phase contrast microscopy (lower row). In the last column, the control experiment was performed with DOPE alone.

copy. As shown in Figure 3a, transfection carried out in the presence of 20 μM **4G4Oct-*cone*** is efficient. At lower calixarene concentration, no transfected cells can be detected, whereas at a concentration of 40 μM, calixarene causes almost complete cell death. A similar behavior is observed with calixarene **4G4Hex-*cone***. Conversely, under the same experimental conditions, no transfection was observed with the conformationally mobile calixarenes **6G6Me-*mobile*** and **8G8Me-*mobile*** and with the conformationally blocked **4G4Pr-*alt*** and **4G4Pr-*cone***. No DNA transfection is observed in the case of calixarenes **4G4Me-*mobile*** (data not shown). For these calixarene derivatives not showing transfection, we then performed experiments in the presence of DOPE (dioleoyl-L-α-phosphatidylethanolamine), a neutral phospholipid commonly used as a transfection adjuvant.[35] In the presence of DOPE, **4G4Pr-*cone*** shows cell transfection (Figure 3b), and at a **4G4Pr-*cone***/DOPE ratio of 1:2, the transfection efficiency is comparable to that of **4G4Oct-*cone*** and **4G4Hex-*cone*** alone. On the other hand, the presence of DOPE does not increase the transfection efficiency of **4G4Oct-*cone*** and **4G4Hex-*cone*** (data not shown). Likewise, DOPE confers transfection ability to the **4G4Me-*mobile*** and **4G4Pr-*alt*** calixarenes, whereas it has no effect on the **6G6Me-*mobile*** and **8G8Me-*mobile*** calixarenes (data not shown).

Interestingly, neither DNA binding nor cell transfection (even in the presence of DOPE) was observed with a cone calix[4]-arene having four propyl groups at the lower rim and four glucose units at the upper rim[36] (data not shown). This corroborates the importance of the guanidinium groups in the DNA condensation process, and it rules out the possibility that DNA delivery to cells is due to a generalized lipophilic effect of the macrocycle.

Discussion

Very few reports exist in the literature on the correlation between DNA condensation and the structure of synthetic vectors used in cell transfection.[37] These studies are almost nonexisting if one refers to macrocyclic compounds, although some of them have been shown to bind nucleic acids.[9,38,39]

(35) Liu, F.; Yang, J.; Huang, L.; Liu, D. *Pharm. Res.* **1996**, *13*, 1642−1646.
(36) Sansone, F.; Casnati, A.; Chierici, E.; Ungaro, R. *Org. Biomol. Chem.* **2003**, *1*, 1802−1809.
(37) Tranchant, I.; Thompson, B.; Nicolazzi, C.; Mignet, N.; Scherman, D. *J. Gene Med.* **2004**, *6*, S24−S35.
(38) Shi, Y.; Schneider, H.-J. *J. Chem. Soc., Perkin Trans. 2* **1999**, *8*, 1797−1803.

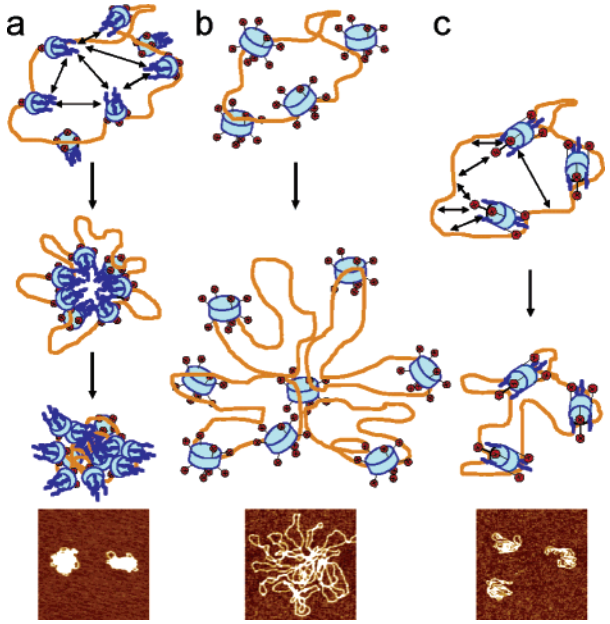

Figure 4. Schematic representation of possible condensation processes induced by (a) the cone guanidinium calix[4]arenes, (b) the conformationally mobile calix[6]- and calix[8]arenes, and (c) the 1,3-alternate and the mobile calix[4]arenes. At the bottom, the AFM images of the aggregates are shown.

The results obtained in the present study clearly indicate that macrocyclic guanidinium calixarenes bind to DNA, condense it, and perform cell transfection in a way which depends on the size, lipophilicity, and conformational properties of the macrocycle. All macrocycles we have tested can be organized into three groups: (i) cone calix[4]arenes, (ii) conformationally mobile calix[6]- and calix[8]arenes, and (iii) 1,3-alternate calix[4]arenes.

To the cone calix[4]arenes group belong compounds **4G4Pr-*cone***, **4G4Hex-*cone***, and **4G4Oct-*cone*** which behave similarly by efficiently condensing both plasmid and linear DNA in a concentration-dependent fashion. These compounds expose the four guanidinium groups from the same side of the macrocyclic ring, and it is quite reasonable that these groups first interact with the negatively charged DNA helix (Figure 4a). The increased local concentration of the calixarenes favors the hydrophobic interaction of the lipophilic tails of DNA-bound calixarenes which join different portions of the DNA molecule thus determining the formation of intramolecular condensates. This mode of interaction is in agreement with the inhibition of DNA condensation by cone guanidinium calix[4]arenes observed in the presence of an increasing amount of ethanol which disrupts hydrophobic interactions. Efficiency in DNA condensation by calix[4]arenes depends on the length of alkyl chains at the lower rim. This picture is supported by the ^{1}H NMR studies of **4G4Hex-*cone*** in D_2O, which prove that this compound is indeed hydrophobically self-associated although at concentrations higher than 0.2 mM. DNA condensation instead takes place at micromolar calixarene concentrations indicating that the self-association process of DNA-bound macrocycles is more efficient due to the higher local concentration of the ligand. The intramolecular DNA condensation mode shown by cone guanidinium calix[4]arenes is the most effective with respect to cell transfection. In fact, only the most lipophilic **4G4Oct-*cone*** and **4G4Hex-*cone*** calixarenes are able to perform cell transfection at a concentration of 15−20 μM. The less lipophilic **4G4Pr-*cone*** promotes transfection only in the presence DOPE, a neutral phospholipid which destabilizes the membrane bilayer. The concentration of the calixarene needed for transfection is higher compared to that required for the formation of the DNA blobs visualized by AFM which are evidently still partially negatively charged for adhering to the mica surface. This higher calixarene concentration would be required for a complete charge neutralization of DNA which becomes a fatty aggregate capable to cross the cell membrane. In line with this hypothesis is the observation that a high calixarene concentration prevents deposition of the aggregates onto the hydrophilic mica surface.

The conformationally mobile **6G6Me-*mobile*** and **8G8Me-*mobile*** calixarenes are larger and more flexible macrocycles compared to calix[4]arene derivatives. They are highly water soluble and do not self-aggregate in a concentration range 4×10^{-3} to 1×10^{-2} M[17] mainly because they bear short methyl groups at the lower rim. Differently from the cone calix[4]arenes described above, they do not form intramolecular DNA condensates but simultaneously interact with several DNA filaments giving rise to intermolecular aggregates composed of many plectomenes linked by interstrand connections (Figure 4b). In this case, the aggregation process is dominated by electrostatic interactions between the positively charged guanidinium groups of the calixarenes and the negatively charged DNA backbone as suggested by the negligible effect of ethanol addition on DNA binding. Supported by the available data on the conformational properties of calix[6]- and calix[8]arene derivatives,[40] we can assume that the guanidinium groups of these macrocycles are oriented in opposite directions with respect to the plane of the calixarene ring (for example, three or four up and three or four down). In this arrangement, the calixarene could efficiently cross-link different DNA molecules generating the gorgonlike aggregates observed by AFM. On the basis of the fact that these large mobile calixarenes favor the melting of DNA (Supporting Information, Figure S5), we cannot rule out that formation of these large multimeric aggregates could partly arise from a kind of macrocycle-mediated strand exchange among different plasmids. The poor DNA condensation achieved with **6G6Me-*mobile*** and **8G8Me-*mobile*** calixarenes explains the reason they are unable to perform cell transfection at any tested concentration and even in the presence of DOPE.

The **4G4Me-*mobile*** and **4G4Pr-*alt***, which have in solution a 1,3-alternate conformation, show an intermediate behavior because they condense DNA, but in this case, the process is driven by charge−charge interactions (Figure 4c) between the guanidinium groups of a calixarene and phosphate groups along the same plasmid, being DNA condensation independent or even enhanced by ethanol. The inability of both compounds to promote transfection can be related to their poor lipophilicity caused in particular by the 1,3-alternate conformation. In line with this hypothesis is the observation that their transfection efficiency is enhanced by the adjuvant DOPE.

Conclusion

By using a combination of spectroscopic techniques and direct visualization by AFM, we have investigated the DNA binding

(39) Zadmard, R.; Schrader, T. *Angew. Chem., Int. Ed.* **2006**, *45*, 2703−2706.

(40) Casnati, A.; Della Ca', N.; Fontanella, M.; Sansone, F.; Ugozzoli, F.; Ungaro, R.; Liger, K.; Dozol, J.-F. *Eur. J. Org. Chem.* **2005**, 2338−2348.

and condensation properties of guanidinium calixarenes and correlated them with their cell transfection ability. The results indicate that relatively small variations in size, lipophilicity, and conformation of these water-soluble compounds, together with a subtle interplay between hydrophobic and electrostatic supramolecular interactions, significantly affect the outcome of DNA condensation and cell transfection. The present study contributes to a better understanding of the factors affecting DNA delivery at the molecular level and may help to design more efficient and safer vectors for gene therapy.

Experimental Section

Synthesis and Characterization of the Guanidinium Calixarenes. All moisture-sensitive reactions were carried out under a nitrogen atmosphere. All dry solvents were prepared according to standard procedures and stored over molecular sieves. Melting points were determined on an electrothermal apparatus in capillaries sealed under nitrogen. ^{1}H and ^{13}C NMR spectra (300 and 75 MHz, respectively) were recorded on a Bruker AV300 spectrometer (partially deuterated solvents were used as internal standards). Mass spectra were recorded in ESI mode on a single quadrupole Micromass ZMD instrument (capillary voltage = 3 kV, cone voltage = 30−160 V, extractor voltage = 3 V, source block temperature = 80 °C, desolvation temperature = 150 °C, cone and desolvation gas (N_2) flow rates = 1.6 and 8 L/min, respectively). TLC was performed on Merck 60 F_{254} silica gel and flash chromatography on 32−63 μm on 60 Å Merck silica gel. Elemental analyses were performed using a CHN 1106 Carlo Erba instrument and are reported as a percentage.

5,11,17,23-Tetra-*tert*-butyl-25,26,27,28-tetrahexyloxycalix[4]arene cone (**1a**),[18] 5,11,17,23-tetra-*tert*-butyl-25,26,27,28-tetrapropoxycalix-[4]arene 1,3-alternate (**1b**),[20] 5,11,17,23-tetra-*tert*-butyl-25,26,27,28-tetramethoxycalix[4]arene mobile (**1c**),[19] 5,11,17,23-tetranitro-25,26,-27,28-tetrahexyloxycalix[4]arene cone (**2a**),[18] and 5,11,17,23-tetramino-25,26,27,28-tetrapropoxycalix[4]arene 1,3-alternate (**3b**)[21] were synthesized according to the literature procedures.

5,11,17,23-Tetra-*tert*-butyl-25,26,27,28-tetrapropoxycalix[4]-arene 1,3-Alternate (1b). The reaction conditions used for the synthesis of this compound are according to the literature,[20] but differently from this previously reported procedure, we found, for the isolation of the pure product, the crystallization from CH_2Cl_2/petroleum ether to be very convenient. The reported separation with column chromatography on silica gel did not give the desired results, recovering the desired product always accompanied by the isomer in partial cone conformation. All the physicochemical data obtained were in accordance with those previously reported.[20]

5,11,17,23-Tetranitro-25,26,27,28-tetrahexyloxycalix[4]arene (2a). **1a** (3 g, 3.04×10^{-3} mol) and $NaNO_3$ (10.3 g, 0.12 mol) were put into a round-bottom flask, and then CF_3COOH (14 mL, 0.18 mol) was added dropwise. The mixture was stirred at rt overnight. The reaction was stopped by addition of water (200 mL) and extracted with CH_2Cl_2 (2×100 mL). The organic layer was washed with water (150 mL) and dried over anhydrous $MgSO_4$. The solvent was removed under reduced pressure, and the pure product was obtained by trituration with MeOH (50 mL) as a pale yellow powder (2.3 g, 81%). Mp: 182−183 °C (MeOH). ^{1}H NMR (300 MHz, $CDCl_3$) δ 7.57 (s, 8H, Ar*H*), 4.51 (d, J = 14.0 Hz, 4H, ArCH_2Ar), 3.98 (t, J = 7.4 Hz, 8H, OCH_2(CH$_2$)$_4$-CH$_3$), 3.40 (d, J = 14.1 Hz, 4H, ArCH_2Ar), 1.87 (m, 8H, OCH$_2$CH_2-(CH$_2$)$_3$CH$_3$), 1.36 (bs, 24H, O(CH$_2$)$_2$(CH_2)$_3$CH$_3$) 0.92 (t, J = 6.9 Hz, 12H, O(CH$_2$)$_5$CH_3). ^{13}C NMR (75 MHz, $CDCl_3$) δ 161.6, 142.8, 135.4, 123.9, 76.2, 31.8, 31.1, 30.1, 25.6, 22.7, 13.9. MS (ESI): calcd for [M + Na]$^+$ m/z = 963.5, found m/z = 963.8. El. anal. calcd for $C_{52}H_{68}N_4O_{12}$: C, 66.36; H, 7.28; N, 5.95. Found: C, 66.19; H, 7.42; N, 5.82.

5,11,17,23-Tetranitro-25,26,27,28-tetrapropoxycalix[4]arene 1,3-Alternate (2b). This compound was prepared with the same procedure as that used for compound **2a** and obtained in 60% yield. Mp: >300 °C (MeOH). ^{1}H NMR (300 MHz, $CDCl_3$) δ 7.96 (s, 8H, ArH), 3.80 (t, J = 7.2 Hz, 8H, OCH_2CH$_2$CH$_3$), 3.73 (s, 8H, ArCH_2Ar), 1.98−1.82 (m, 8H, OCH$_2$CH_2CH$_3$), 1.05 (t, J = 7.5 Hz, OCH$_2$CH$_2$CH_3). ^{13}C NMR (75 MHz, $CDCl_3$) δ 161.4, 142.0, 133.6, 125.7, 74.9, 35.6, 23.6, 10.2. MS (ESI): calcd for [M + Na]$^+$ m/z = 795.3, found m/z = 795.1. El. anal. calcd for $C_{40}H_{44}N_4O_{12}$: C, 62.17; H, 5.74; N, 7.25. Found: C, 62.30; H, 5.61; N, 7.12.

5,11,17,23-Tetranitro-25,26,27,28-tetramethoxycalix[4]arene (2c). This compound was prepared with the same procedure as that used for compound **2a** and obtained in 75% yield. In $CDCl_3$, it is present in a mixture of partial cone (90% ca.) and cone (10% ca.) conformers. Mp: 296−298 °C (MeOH). ^{1}H NMR (300 MHz, $CDCl_3$) δ 8.23 (s, 1.8H, ArH, partial cone), 8.14 (s, 1.8H, ArH, partial cone) 7.86 (d, J = 3.0 Hz, 1.8H, ArH, partial cone), 7.70 (s, 0.8H, ArH, cone), 7.27 (d, J = 3.0 Hz, 1.8H, ArH, partial cone), 4.43 (d, J = 13.2 Hz, 0.4H, ArCH_2-Ar, cone), 4.10 (d, J = 13.8 Hz, 1.8H, ArCH_2Ar, partial cone), 3.92 (s, 3.6H, ArCH_2Ar, partial cone), 3.86 (s, 1.2H, OCH$_3$, cone), 3.84 (s, 2.7H, OCH$_3$, partial cone), 3.83 (s, 8.1H, OCH$_3$, partial cone), 3.46 (d, J = 13.2 Hz, 0.4H, ArCH_2Ar, cone), 3.37 (d, J = 13.8 Hz, 1.8H, ArCH_2-Ar, partial cone). MS (ESI): calculated for [M + Na]$^+$ m/z = 683.2, found m/z = 683.1. El. anal. calcd for $C_{32}H_{28}N_4O_{12}$: C, 58.18; H, 4.27; N, 8.48. Found: C, 58.33; H, 4.41; N, 8.34.

5,11,17,23-Tetramino-25,26,27,28-tetrahexyloxycalix[4]arene (3a). To a suspension of **2a** (500 mg, 5.31×10^{-4} mol) in ethanol (10 mL) were added $NH_2NH_2 \cdot H_2O$ (0.52 mL, 1.06×10^{-2} mol) and Pd/C (10%) (catalytic amount). The reaction mixture was refluxed and stirred overnight. The catalyst was filtered off through a paper filter. The paper filter was washed with CH_2Cl_2 (20 mL), and all solvents were removed under reduced pressure. The residue was dissolved in CH_2Cl_2 (30 mL) and dried over $MgSO_4$. The pure product was obtained after evaporation of the solvent as a pale brown powder in 95% yield. Mp: 234−236 °C. ^{1}H NMR (300 MHz, $CDCl_3$) δ 6.08 (s, 8H, Ar*H*), 4.34 (d, J = 13.1 Hz, 4H, ArCH_2Ar), 3.78 (t, J = 7.4 Hz, 8H, OCH_2(CH$_2$)$_4$CH$_3$), 3.24 (bs, 8H, ArNH_2), 2.94 (d, J = 13.1 Hz, 4H, ArCH_2Ar), 1.88 (m, 8H, OCH$_2$CH_2(CH$_2$)$_3$CH$_3$), 1.38 (bs, 24H, O(CH$_2$)$_2$(CH_2)$_3$CH$_3$), 0.94 (t, J = 6.6 Hz, 12H, O(CH$_2$)$_5$CH_3). ^{13}C NMR (75 MHz, $CDCl_3$) δ 150.0, 140.1, 135.6, 115.7, 75.9, 32.1, 31.1, 30.1, 25.9, 22.8, 14.1. MS (ESI): calcd for [M + Na]$^+$ m/z = 843.6, found m/z = 843.9. El. anal. calcd for $C_{52}H_{76}N_4O_4$: C, 76.06; H, 9.33; N, 6.82. Found: C, 76.23; H, 9.08; N, 6.94.

5,11,17,23-Tetramino-25,26,27,28-tetrapropoxycalix[4]arene 1,3-Alternate (3b). This compound was prepared with the same procedure as that used for compound **3a** starting from **2b** and obtained in 95% yield. All the physicochemical data were in accordance with those previously reported.[21]

5,11,17,23-Tetramino-25,26,27,28-tetramethoxycalix[4]arene (3c). This compound was prepared with the same procedure as that used for compound **3a** starting from **2c** and obtained in 90% yield. Mp: 211 °C, dec. ^{1}H NMR (300 MHz, 373 K, DMSO-d_6) δ 6.15 (s, 8H, Ar*H*), 4.12 (bs, 8H, NH$_2$), 3.40 (bs, 12H, OCH$_3$), 3.06 (bs, 8H, ArCH_2Ar). ^{13}C NMR (75 MHz, DMSO-d_6) δ 148.9, 142.3, 133.9, 114.2, 60.7, 30.5. MS (ESI): calcd for [M + Na]$^+$ m/z = 563.3, found m/z = 563.4. El. anal. calcd for $C_{32}H_{36}N_4O_4$: C, 71.09; H, 6.71; N, 10.36. Found: C, 70.89; H, 6.93; N, 10.22.

5,11,17,23-Tetrakis[(bis-*N*-Boc)guanidine]-25,26,27,28-tetra-hexyloxycalix[4]arene Cone (4a). To a solution of **3a** (328 mg, 4×10^{-4} mol), bis-Boc-thiourea (464 mg, 1.68×10^{-3} mol), and Et_3N (0.84 mL, 6×10^{-3} mol) in dry CH_2Cl_2 (20 mL), cooled with an ice bath, was added 2-chloro-1-methyl-pyridinium iodide (729 mg, 2.80×10^{-3} mol), and the mixture was stirred for 30 min. The cooling bath was removed, and the reaction mixture was stirred at rt overnight. The organic solvent was distilled off under reduced pressure, and the residue was purified by flash column chromatography on silica gel (eluent: hexane/Et_2O 5:1 and 7:3) to obtain the pure product as a white powder in 31% yield. Mp: >250 °C dec (CH_2Cl_2−MeOH). ^{1}H NMR (300

MHz, $CDCl_3$) δ 11.59 (s, 4H, BocN*H*), 9.80 (s, 4H, ArN*H*), 6.90 (s, 8H, Ar*H*), 4.40 (d, $J = 13.1$ Hz, 4H, ArCH_2Ar), 3.83 (t, $J = 7.5$ Hz, 8H, OCH_2(CH_2)$_4$$CH_3$), 3.13 (d, $J = 13.1$ Hz, 4H, ArCH_2Ar), 1.90 (m, 8H, $OCH_2CH_2(CH_2)_3CH_3$), 1.48 (s, 36H, Bu^t), 1.45 (s, 36H, Bu^t), 1.36 (m, 24H, O(CH_2)$_2$(CH_2)$_3$$CH_3$), 0.92 (t, $J = 6.3$ Hz, 12H, O(CH_2)$_5$$CH_3$). ^{13}C NMR (75 MHz, $CDCl_3$) δ 153.9, 153.4, 153.0, 134.7, 130.6, 123.0, 83.0, 79.1, 75.4, 32.1, 31.3, 30.1, 28.2, 28.1, 25.9, 22.8, 14.1. MS (ESI): calcd for $[M + Na]^+$ $m/z = 1812.1$, found $m/z = 1812.3$. El. anal. calcd for $C_{96}H_{148}N_{12}O_{20}$: C, 64.40; H, 8.33; N, 9.39. Found: C, 64.67; H, 8.57; N, 9.17.

5,11,17,23-Tetrakis[(*N*,*N*′-di-Boc)guanidine]-25,26,27,28-tetrapropoxycalix[4]arene 1,3-Alternate (4b). To a solution of **3b** (273 mg, 4.18×10^{-4} mol), *N*,*N*′-di-Boc-thiourea (463 mg, 1.67×10^{-3} mol), and Et_3N (0.59 mL, 4.18×10^{-3} mol) in dry DMF (15 mL), cooled with an ice bath, was added mercury chloride (510 mg, 1.84×10^{-3} mol), and the mixture was stirred for 30 min. The cooling bath was removed, and the reaction mixture was stirred at rt overnight. The reaction mixture was diluted with CH_2Cl_2 (10 mL), and the black solid phase of HgS was filtered off through a paper filter. The filtrate was distilled off under reduced pressure, and the residue was purified by flash column chromatography on silica gel eluting with ethyl acetate/hexane 3:1 to obtain the pure product as a white solid in 64% yield. Mp: >250 °C dec. ^{1}H NMR (300 MHz, $CDCl_3$) δ 11.61 (s, 4H, BocN*H*), 10.16 (s, 4H, ArN*H*), 7.31 (s, 8H, Ar*H*), 3.56 (t, $J = 6.3$ Hz, 8H, OC$H_2$$CH_2CH_3$), 3.51 (s, 8H, ArC$H_2$Ar), 1.78 (m, 8H, OCH_2CH_2-CH_3), 1.54 (s, 36H, Bu^t), 1.46 (s, 36H, Bu^t), 1.07 (t, $J = 7.3$ Hz, 12H, $OCH_2CH_2CH_3$). ^{13}C NMR (75 MHz, $CDCl_3$) δ 163.4, 153.4, 153.1, 152.9, 133.4, 130.1, 123.1, 83.2, 78.7, 73.6, 36.3, 28.1, 27.9, 23.8, 11.2. MS (ESI) calcd for $[M + Na]^+$ $m/z = 1643.9$, found $m/z = 1643.7$. El. anal. calcd for $C_{84}H_{124}N_{12}O_{20}$: C, 62.20; H, 7.71; N, 10.36. Found: C, 62.01; H, 7.95; N, 10.19.

5,11,17,23-Tetrakis[(*N*,*N*′-di-Boc)guanidine]-25,26,27,28-tetramethoxycalix[4]arene Mobile (4c). This compound was obtained with the same procedure as that used to obtain **4b**, but the reaction mixture was stirred at rt for 3 days. The crude was purified by flash column chromatography on silica gel (eluent:ethyl acetate/hexane 5:1 and 4:1) to obtain the pure product as a white solid in 21% yield. Mp: >200 °C dec. ^{1}H NMR (300 MHz, $T = 363$ K, DMSO-d_6) δ 11.33 (brs, 4H, BocN*H*), 9.64 (brs, 4H, ArN*H*), 7.15 (brs, 8H, Ar*H*), 3.17−4.06 (brs, 20H, ArCH_2Ar and OCH_3), 1.49 (s, 36H, Bu^t), 1.37 (s, 36H, Bu^t). ^{13}C NMR (75 MHz, $CDCl_3$) δ 163.6, 155.2, 153.4, 153.1, 134.4, 133.7, 130.8, 123.0, 83.1, 79.0, 61.3, 60.2, 31.1, 28.1, 28.0. MS (ESI): calcd for $[M + Na]^+$ $m/z = 1531.8$, found $m/z = 1531.5$. El. anal. calcd for $C_{76}H_{108}N_{12}O_{20}$: C, 60.46; H, 7.21; N, 11.13. Found: C, 60.71; H, 7.54; N, 10.92.

General Procedure for the Removal of the Boc Protecting Groups. Concentrated HCl was added dropwise to a solution of the protected guanidinium calixarene (**4a**−**c** and **9a**,**b**) in 1,4-dioxane (0.1 mmol/10 mL). The reaction mixture was stirred for 24 h, and then the solvent was removed under reduced pressure.

5,11,17,23-Tetraguanidinium-25,26,27,28-tetrahexyloxycalix[4]arene, Tetrachloride Salt Cone (4G4Hex-*cone*). The crude was triturated with ethyl acetate to obtain the pure product as a white powder in 95% yield. Mp: >250 °C dec. ^{1}H NMR (300 MHz, CD_3OD) δ 6.66 (s, 8H, Ar*H*), 4.49 (d, $J = 13.2$ Hz, 4H, ArCH_2Ar), 3.95 (t, $J = 7.4$ Hz, 8H, OCH_2(CH_2)$_4$$CH_3$), 3.29 (d, $J = 13.2$ Hz, 4H, ArCH_2Ar), 1.98 (m, 8H, $OCH_2CH_2(CH_2)_3CH_3$), 1.45 (m, 24H, O(CH_2)$_2$(CH_2)$_3$$CH_3$), 0.94 (t, $J = 6.3$ Hz, 12H, O(CH_2)$_5$$CH_3$). ^{13}C NMR (75 MHz, CD_3OD) δ 157.8, 157.1, 137.7, 129.9, 126.6, 76.9, 33.4, 31.7, 31.6, 27.4, 24.1, 14.6. MS (ESI): calcd for $[M + H - 4HCl]^+$ $m/z = 989.7$, found $m/z = 989.7$.

5,11,17,23-Tetraguanidinium-25,26,27,28-tetrapropoxycalix[4]arene, Tetrachloride Salt 1,3-Alternate (4G4Pr-*alt*). The pure compound was obtained by crystallization from ethanol/ethyl acetate as a white powder in 87% yield. Mp: >300 °C (EtOH−EtAc). ^{1}H NMR (300 MHz, CD_3OD) δ 7.02 (s, 8H, Ar*H*), 3.82 (t, $J = 7.5$ Hz, 8H, OC$H_2$$CH_2CH_3$), 3.67 (s, 8H, ArC$H_2$Ar), 1.95 (m, 8H, OCH_2CH_2-CH_3), 1.04 (t, $J = 7.4$ Hz, 12H, OCH_2CH_3). ^{13}C NMR (75 MHz, CD_3-OD) δ 158.4, 157.4, 136.5, 129.2, 129.0, 76.9, 36.9, 25.4, 10.9. MS (ESI): calcd for $[M + H - 4HCl]^+$ $m/z = 821.5$, found $m/z = 822.0$.

5,11,17,23-Tetraguanidinium-25,26,27,28-tetramethoxycalix[4]arene, Tetrachloride Salt Mobile (4G4Me-*mobile*). The pure compound was obtained by crystallization from methanol/ethyl as a white powder in 89% yield. Mp: >250 °C dec. ^{1}H NMR (300 MHz, D_2O) δ 7.12 (s, 8H, Ar*H*), 3.73 (s, 8H, ArCH_2Ar), 3.54 (s, 12H, OCH_3). ^{13}C NMR (75 MHz, D_2O) δ 160.1, 158.8, 139.3, 133.1, 131.6, 62.1, 38.5. MS (ESI): calcd for $[M + H - 4HCl]^+$ $m/z = 709.4$, found $m/z = 709.6$.

DNA Preparation and Storage. Plasmid DNA was purified through cesium chloride gradient centrifugation.[41] A stock solution of the plasmid (0.7 μM) in milliQ water (Millipore Corp., Burlington, MA) was stored at −20 °C. Linearized plasmid DNA (pEGFP-C1) was obtained by cutting with the EcoRI restriction enzyme (Roche), column purified (Genomed), and alcohol precipitated. The linearized plasmid DNA pellet was washed with 70% of ethanol, air-dried, and dissolved in distilled H_2O at a final concentration of 1 μg/mL. Linear 1200 bp DNA fragments were obtained from PCR using pDE13 plasmid as the template and suitable DNA primers. The fragment was gel purified on 1% agarose, electroeluted by means of the Elutrap apparatus (Schleicher & Schuell), phenol extracted, and ethanol precipitated. The DNA fragment was dissolved in TE buffer at a concentration of 100 nM and stored at 4 °C.

Sample Preparation and AFM Imaging. DNA samples were prepared by diluting the DNA (plasmid or linear) to a final concentration of 1 nM in deposition buffer (4 mM Hepes, 10 mM NaCl, 2 mM $MgCl_2$, pH = 7.4) either in the presence or in the absence of calixarenes. When needed, ethanol at a defined concentration was added to the deposition buffer prior to addition of DNA and calixarenes. The mixture was incubated for 5 min at room temperature, and then a 20 μL droplet was deposited onto freshly cleaved ruby mica (Ted Pella, Redding, CA) for 1 min. The mica disk was rinsed with milliQ water and dried with a weak stream of nitrogen. AFM imaging was performed on the dried sample with a Nanoscope IIIA Microscope (Digital Instruments Inc., Santa Barbara, CA) operating in tapping mode. Commercial diving board silicon cantilevers (NSC-15 Micromash Corp., Estonia) were used. Images of 512 × 512 pixels were collected with a scan size of 2 μm at a scan rate of 3−4 lines per second and were flattened after recording using Nanoscope software.

Cell Culture and Transient Transfection Assay. The human rhabdomyosarcoma cell line RD-4, obtained from David Derse, National Cancer Institute, Frederick, Maryland, was maintained as a monolayer using growth medium containing 90% DMEM, 10% FBS, 2 mM L-glutamine, 100 IU/mL of penicillin, and 10 μg/mL of streptomycin. Cells were subcultured to a fresh culture vessel when growth reached 70−90% confluence (i.e., every 3−5 days) and incubated at 37 °C in a humidified atmosphere of 95% air/5% CO_2. Transfections were performed in 6 well plates, when cells were 80% confluent (approximately 3×10^5 cells) on the day of transfection. A portion of 3 μg of plasmid and different concentrations of ligands were added to 1 mL of a serum-free medium, mixed rapidly, and incubated at room temperature for 20 min. Each mixture was carefully added to the cells following the aspiration of the culture medium from the cells. Lipoplex formulations were performed adding DOPE to the plasmid−ligand mixture at different ligand/DOPE molar ratios (1:1, 1:2, and 2:1), where ligand concentration was kept to 15 μM. The GenePORTER transfection reagent, a neutral lipid transfection reagent, was used as positive transfection control. The mixture and cells were incubated at 37 °C in a humidified atmosphere of 95% air/5% CO_2 for 5 h. Finally, the

(41) Maniatis, T.; Fritsch, E. F.; Sambrook, J. In *Molecular Cloning: A Laboratory Manual*, 2nd ed.; Cold Spring Harbor Laboratory: New York, 1989.

transfection mixture was removed and 3 mL of growth medium was added to each transfected well and left to incubate for 72 h.

The transfected cells were observed under a fluorescence microscope for EGFP expression.

Acknowledgment. This work was partially supported by EU (CARBONA, HPRN-CT-2002-00190) and by the Ministero dell'Istruzione, Università, Ricerca (MIUR), FIRB project RBNE019H9K: Manipolazione Molecolare per Macchine Nanometriche, FIRB project RBNE01KMT9, and PRIN project 2005, 2005078885. We thank CIM (Centro Interdipartimentale Misure) of the University of Parma for NMR and AFM facilities.

Supporting Information Available: Figures S1−S8, ^{1}H NMR spectra of compounds **4G4Hex-*cone***, **4G4Pr-*alt***, **4G4Me-*mobile***, **2G4Oct-*cone***, and **3G4Oct-*cone***, and complete ref 5. This material is available free of charge via the Internet at http://pubs.acs.org.

JA0634425